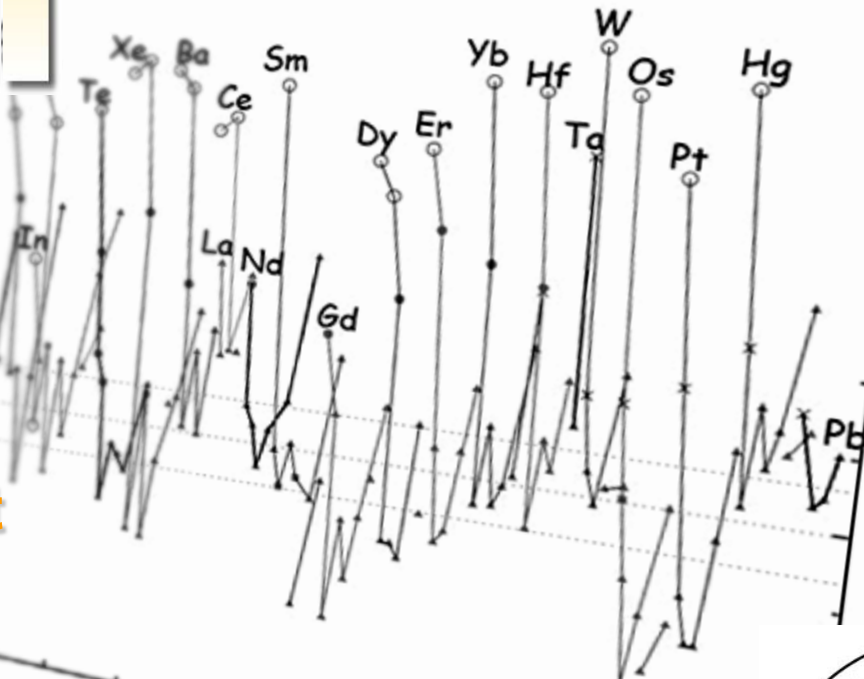


Vanadium	Cr	Mn	Fe	Co
6.1	Chromium 7.19	Manganese 7.43	Iron 7.87	Cobalt 8.08
[Ar]3p ₂	2662 1875	[Ar]3d _{5/2}	[Ar]3d _{5/2}	[Ar]3d _{5/2}
92.91	42	95.94	43	(98)
			44	101.1
Nb	Mo	Tc	Ru	Rh
Tantalum 8.57	Molybdenum 10.22	Technetium (11.487)	Ruthenium 12.2	Rhenium 13.8
[Ar]4d _{5/2}	[Ar]4d _{5/2}	[Ar]4d _{5/2}	[Ar]4d _{5/2}	[Ar]4d _{5/2}
180.95	74	183.85	75	186.2
			76	190.2
Ta	W	Re	Os	Ir

p-process

in multi-D SNIa

ers with $1.5 < T_9 < 3.7$ K, flat s-seed distribution
 $^{56}\text{Fe} = 0.58$



C. Travaglio

Observatory Turin (Italy)

F. Roepke, W. Hillebrandt

MPA Munich (Germany)

R. Gallino

University Turin (Italy)

Computer resources thanks to

s-process

Claudia Travaglio

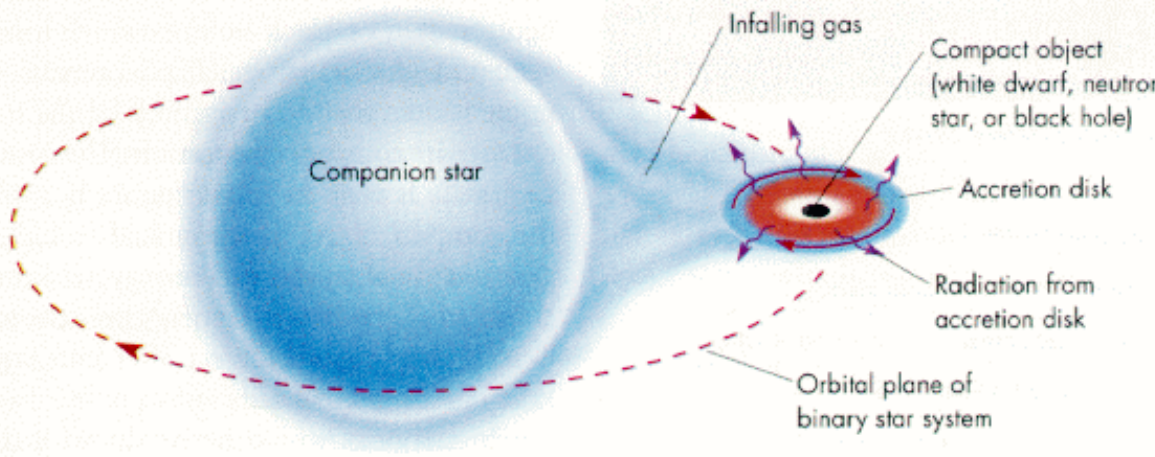
Heidelberg, July 19-23 2010

Vanadium	Cr	Mn	Fe	Co
6.1	Cr	Mn	Fe	Co
92.91	42	95.94	43	(98) M
Nb	Mo	Tc	Ru	Rh
Titanium	Molybdenum	Technetium	Ruthenium	Rhenium
8.57	6.57	0.447	10.3	10.0
180.95	74	183.85	75	186.2
Ta	W	Re	Os	Ru
180.95	74	183.85	75	186.2

Who studied this problem:

*Howard, Meyer, Woosley 199**;
*Arnould, Prantzos 199**;
*Goriely et al. 200**;
*Kusakabe, Iwamoto, Nomoto 201**

s-process in accreted mass



“Accreting white dwarfs as an alternate or additional source of s-process isotopes” (Iben, ApJ 243, 1981)

β -process

Claudia Travaglio

Heidelberg, July 19-23 2010



Hydrogen-accreting CO white dwarf

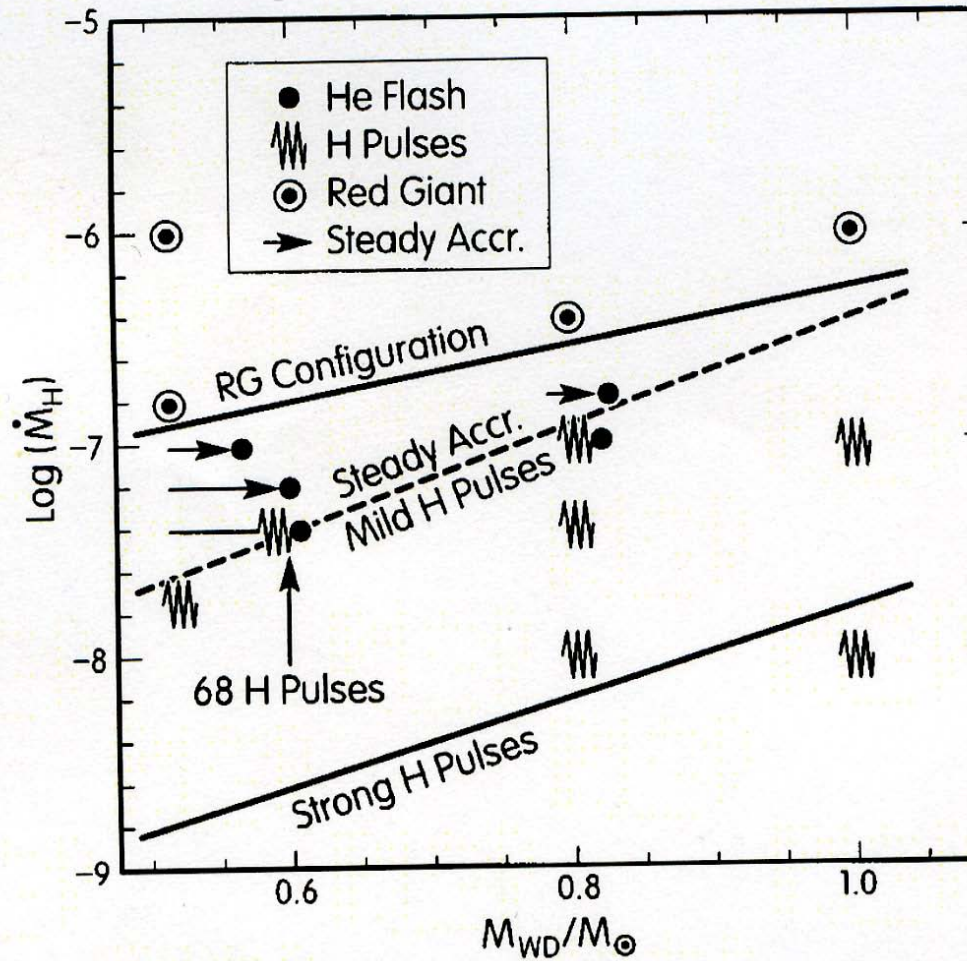


FIG. 10.—Parameter space in the \dot{M} - M_{WD} plane explored in the present work. Various symbols mark the different outcomes experienced by the various computed models, depending on initial white dwarf mass and accretion rate (see the text for symbol meanings). The results of accretion experiments performed by Livio et al. (1989) with a $1 M_{\odot}$ WD are also shown at the right in the figure.

*Cassisi, Iben,
Tornambe' 1998,
ApJ, 496, 376*

*Piersanti, Cassisi,
Iben, Tornambe'
2000, ApJ, 535, 932*

P-process

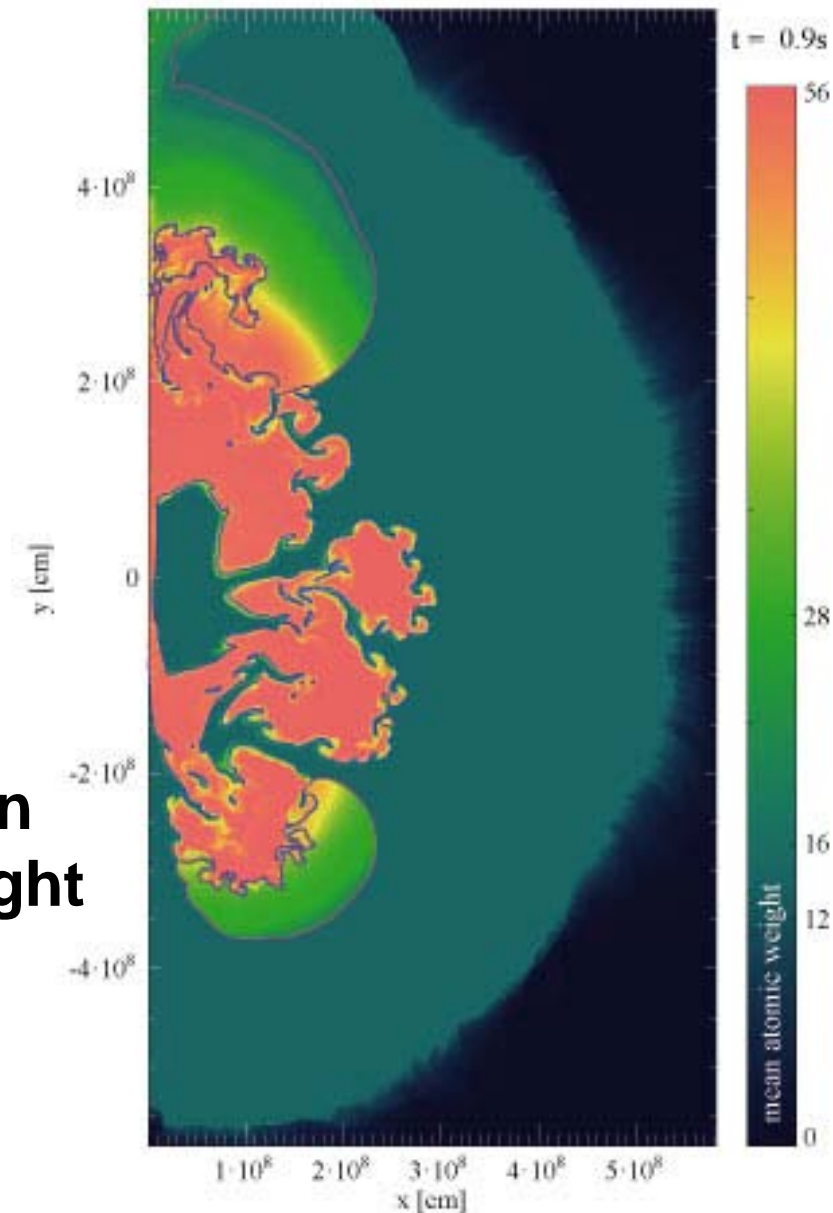
Claudia Travaglio

Heidelberg, July 19-23 2010



Type Ia models: 2D

(simulation done by F. Ropke)



We tested different
SNIa models:

- pure deflagration
- delayed detonation
with different strength

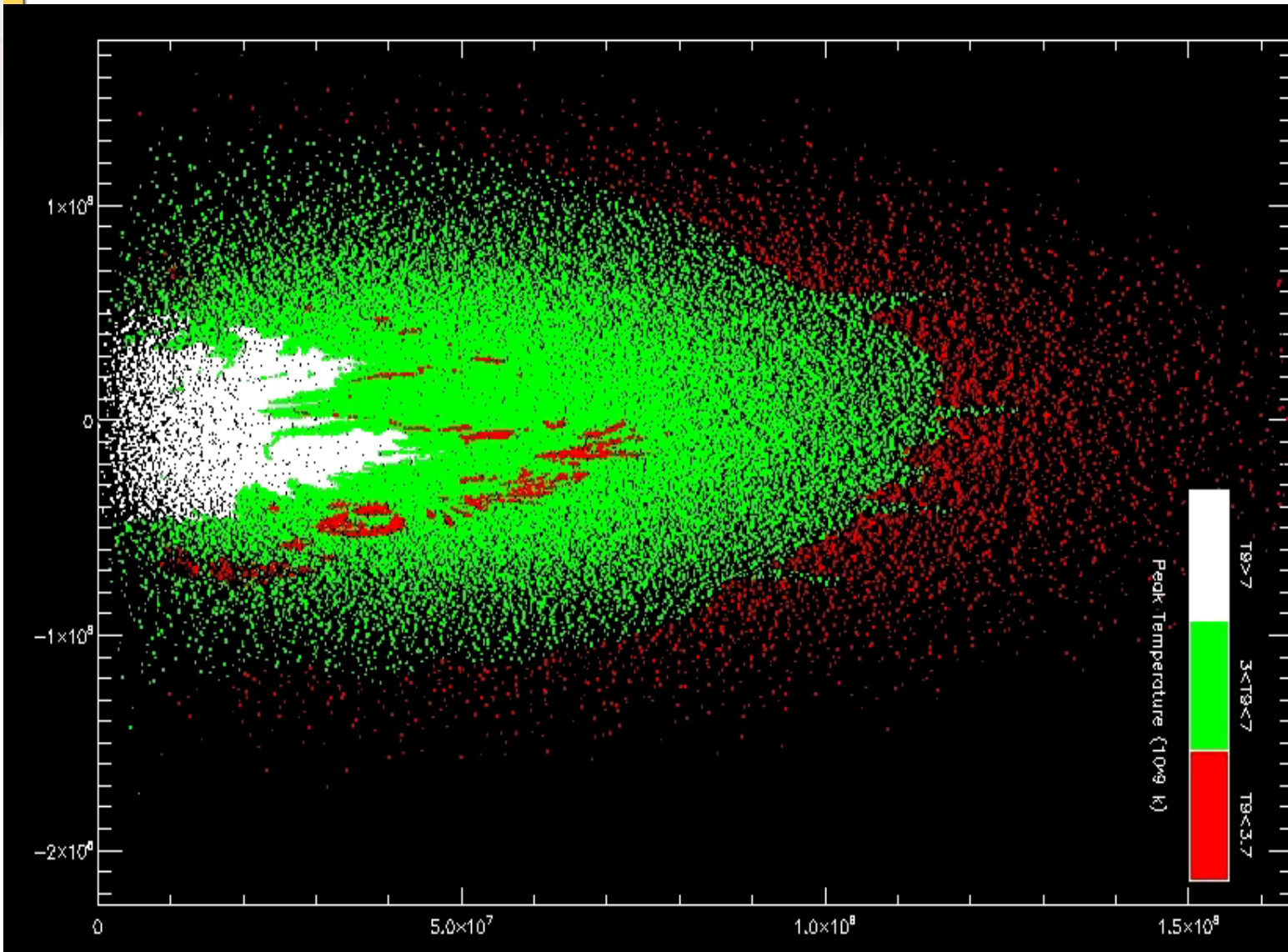
D-process

Claudia Travaglio

Heidelberg, July 19-23 2010

Vanadium	Cr	Mn	Fe	Co
6.1	Chromium	Manganese	Iron	Cobalt
4	Atomic No.	Atomic No.	Atomic No.	Atomic No.
92.91	42	59.94	43	58.93
Nb	Mo	Tc	Ru	Rh
Niobium	Molybdenum	Technetium	Ruthenium	Rhenium
8.57	10.22	0.437	10.3	10.18
180.95	74	183.85	75	186.2
Ta	W	Re	Os	Ir
Tantalum	Wolfram	Rhenium	Osmium	Iridium
10.87	10.22	10.437	10.3	10.18
180.95	74	183.85	75	186.2

Tracer particles in SNIa models



p-process

Claudia Travaglio

Heidelberg, July 19-23 2010



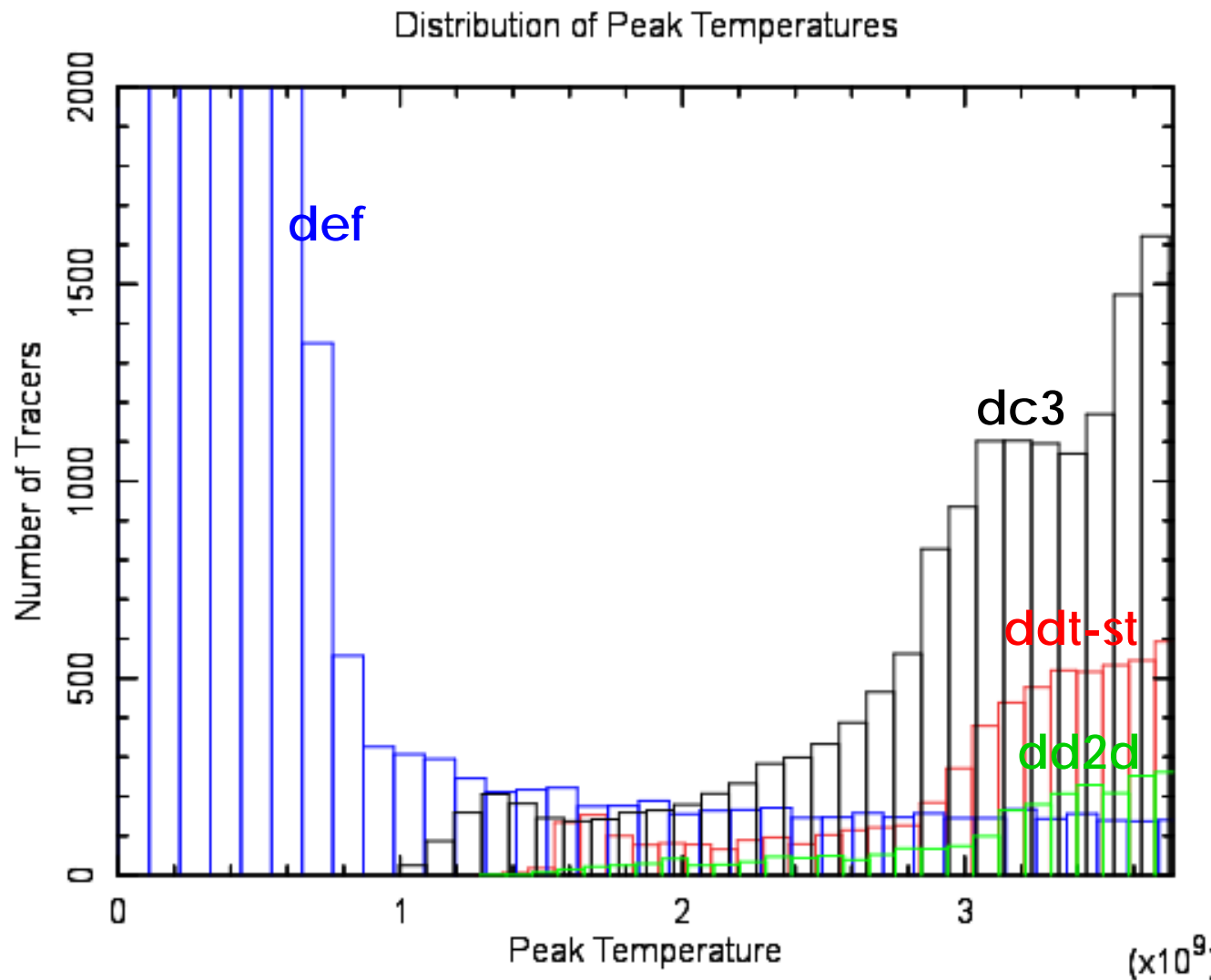
Distribution of tracers

def = deflagration

ddt-st = standard del. det.

dc3 = weaker del. det.

dd2d = stronger del. det.



P-process

Claudia Travaglio

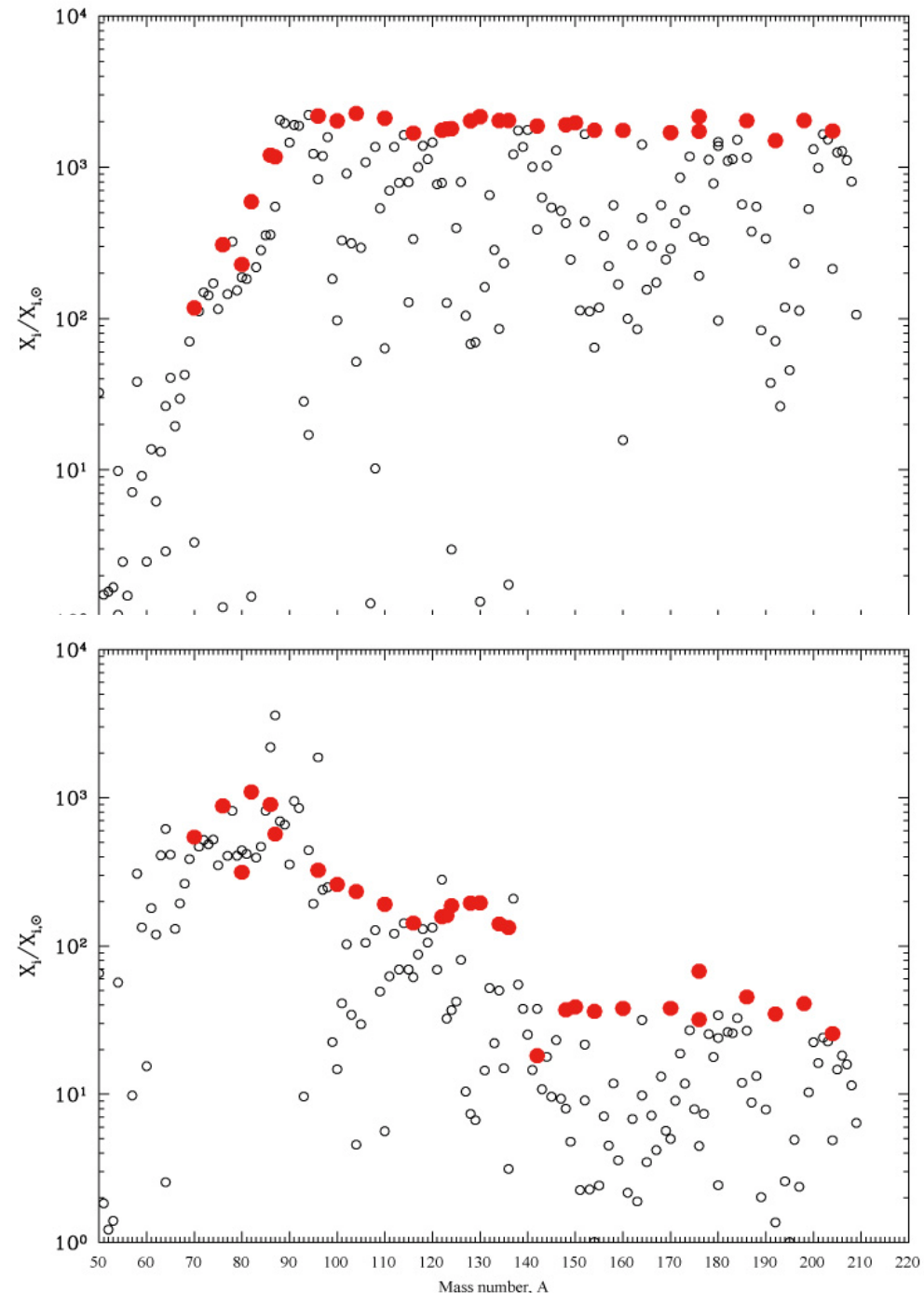
Heidelberg, July 19-23 2010



s-process seeds

Preliminary
s-process tests
in a close
binary system
during the
secondary
companion
MS/giant
accreting
on a WD

(*Cristallo,
Piersanti et al.
in progress*)



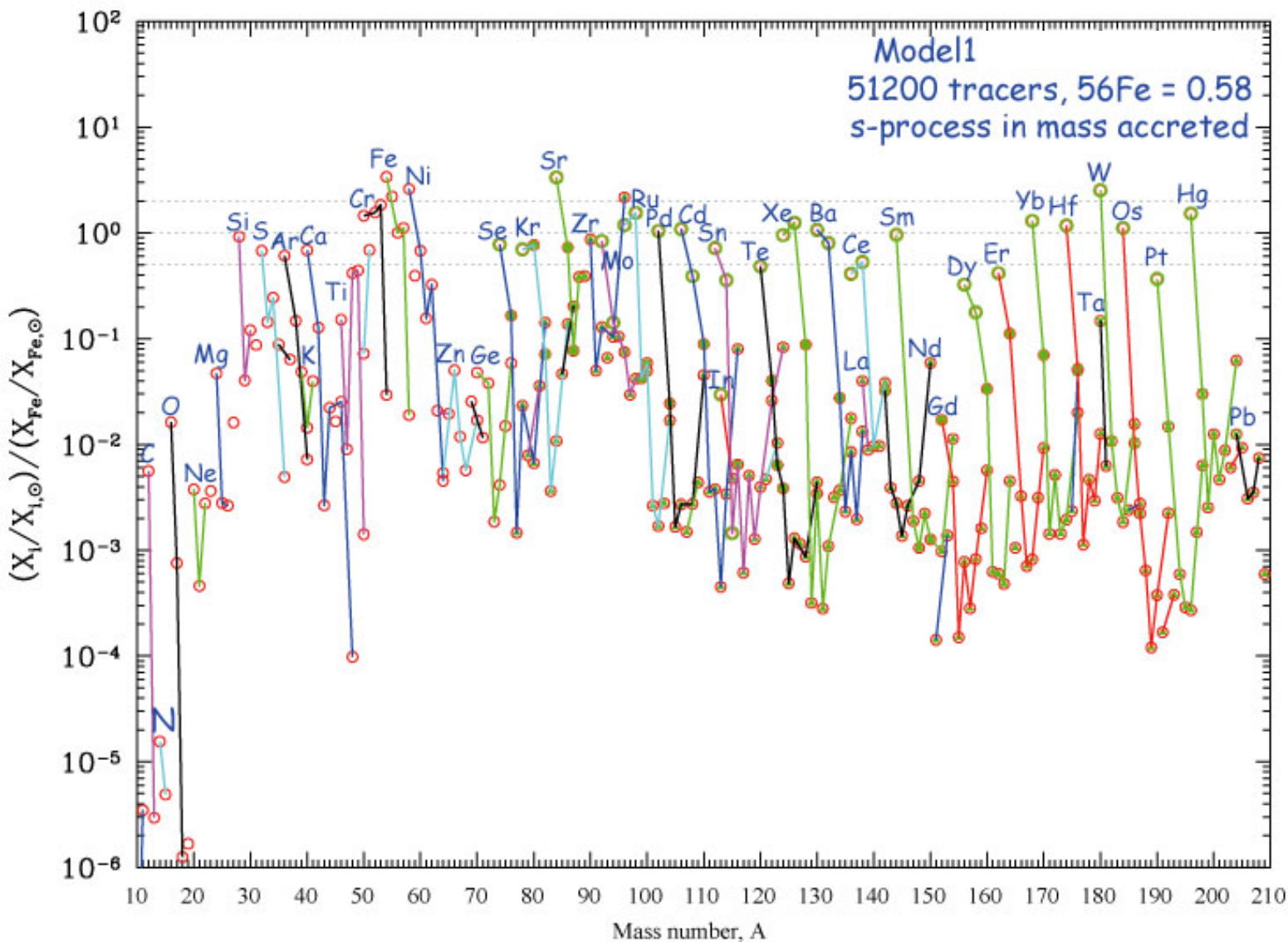
s-process

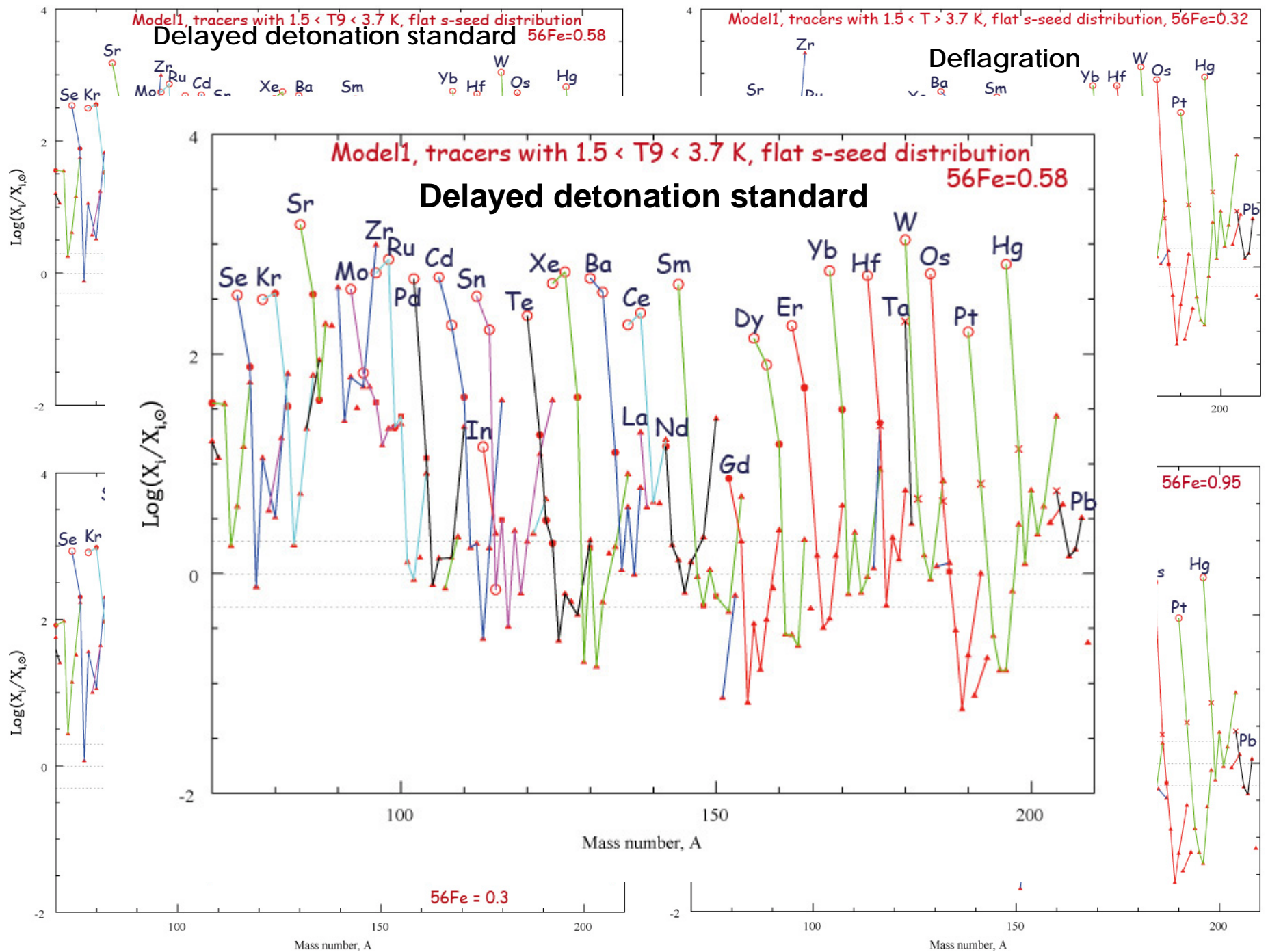
Claudia Travaglio

Heidelberg, July 19-23 2010



Results: solar metallicity

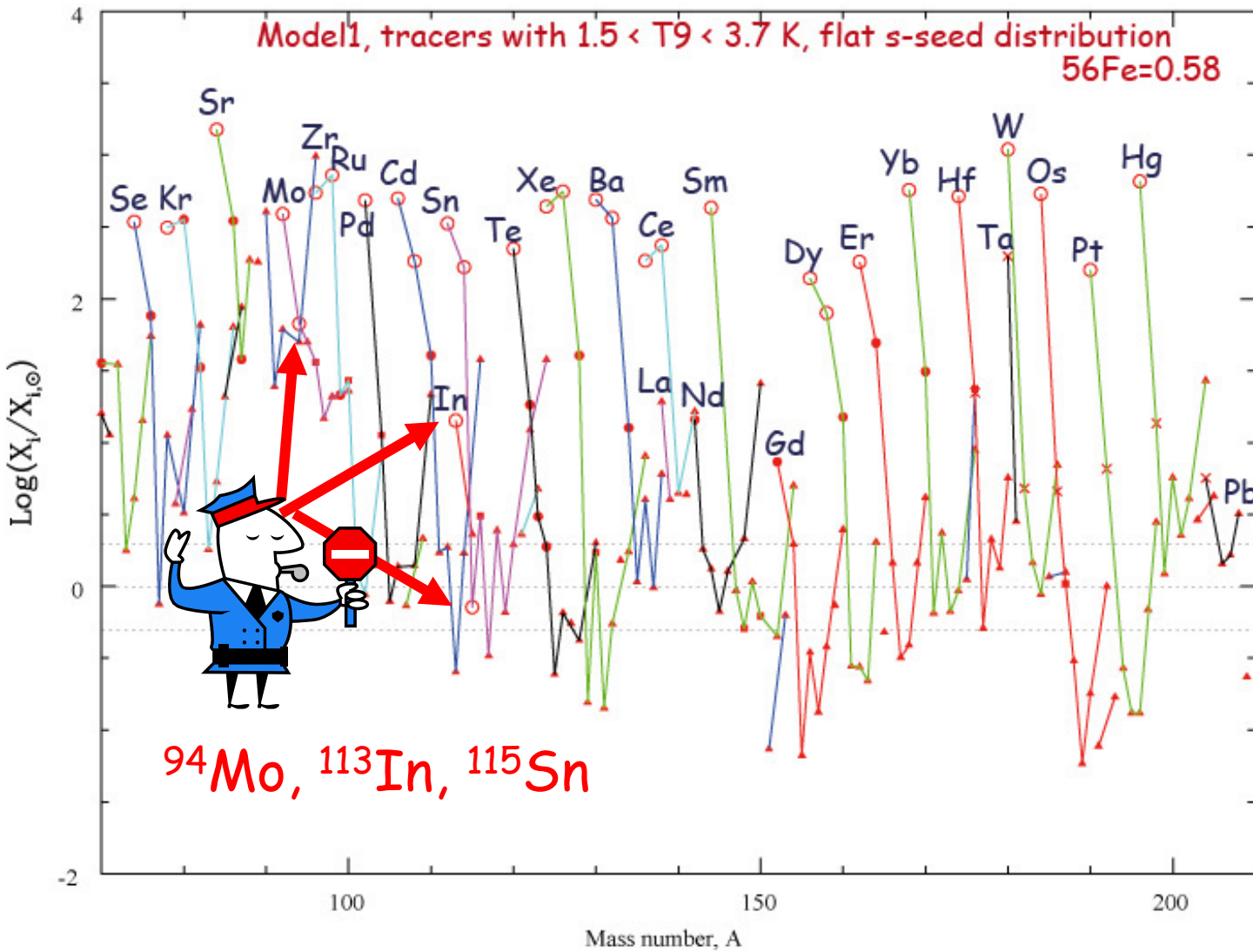




p-process

Claudia Travaglio

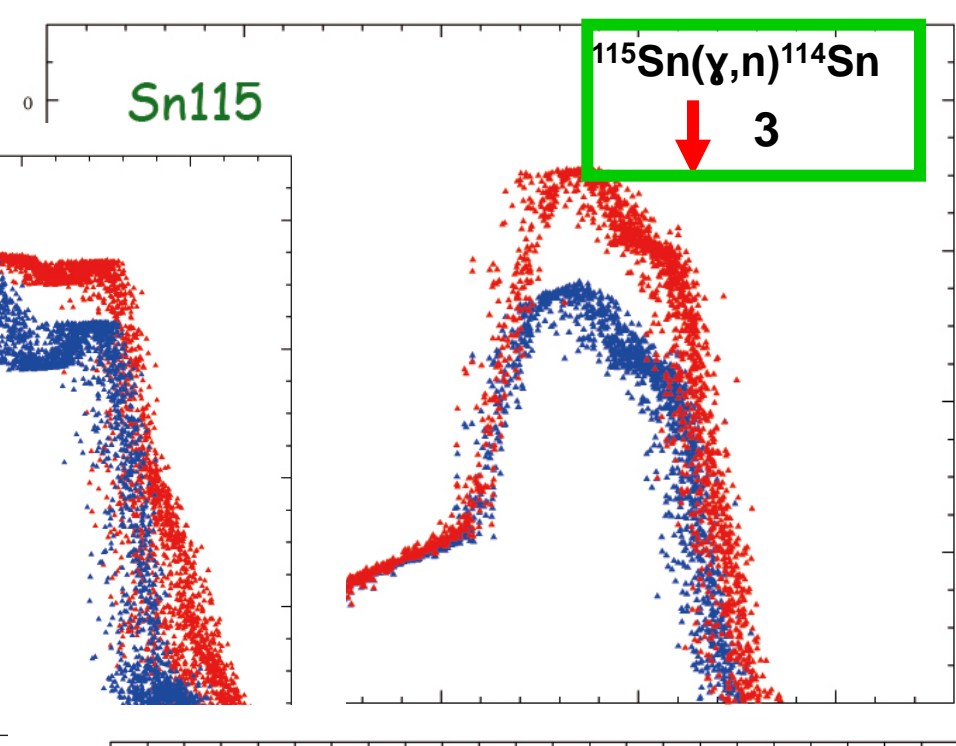
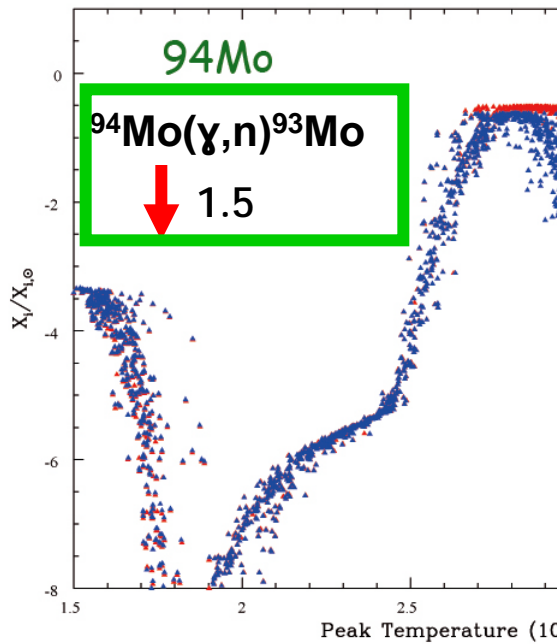
Heidelberg, July 19-23 2010



p-process

Claudia Travaglio

Heidelberg, July 19-23 2010

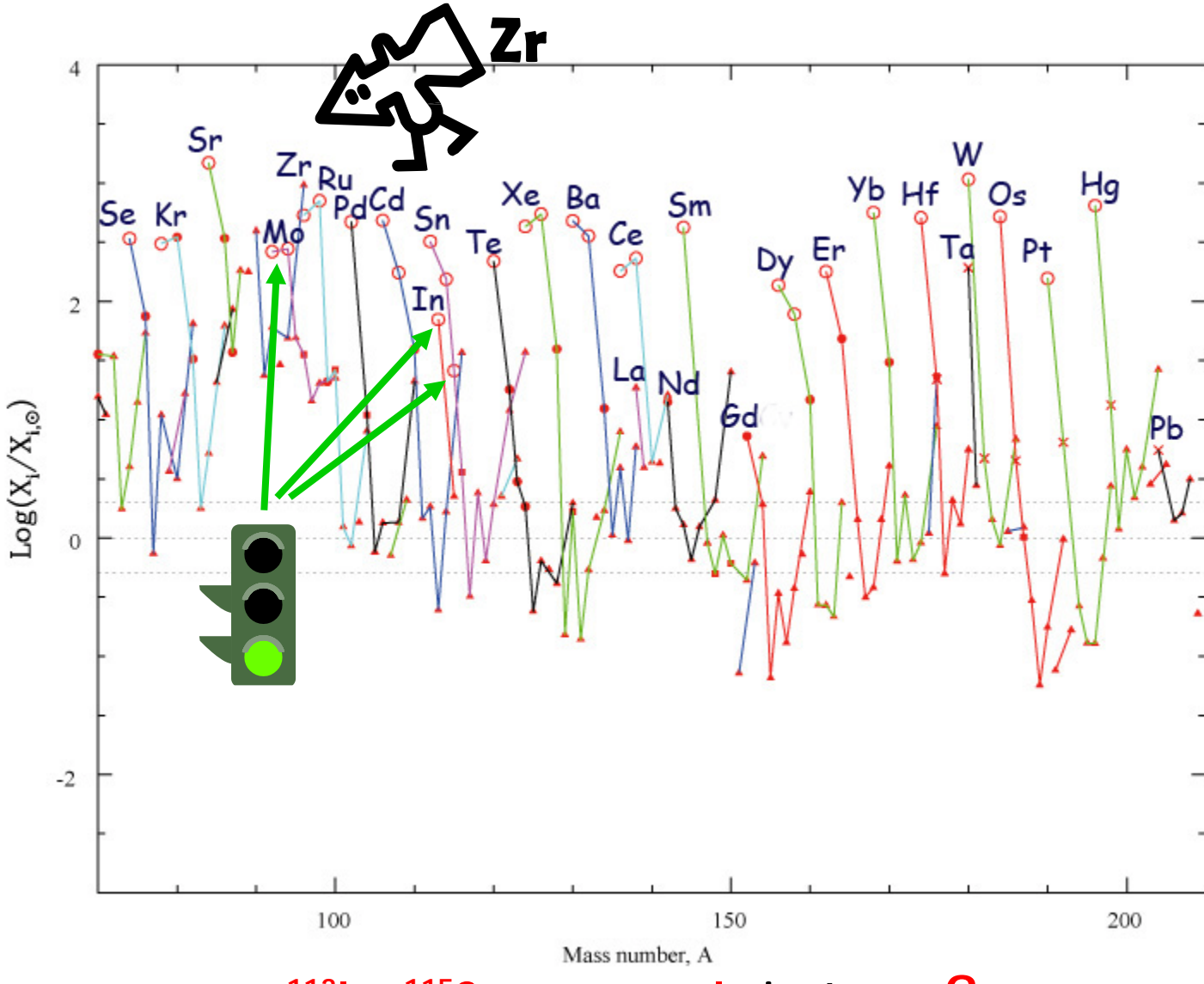


b-process

Claudia Travaglio

Heidelberg, July 19-23 2010

V	Niobium 6.1	Cr	Manganese 7.43	Mn	Iron 7.87	Co
Ta	Technetium 8.57	Mo	Neodymium 10.22	Tc	Ruthenium 11.3	Rh
W	180.95	74	183.85	75	186.2	190.2
Ta	Technetium 8.57	Mo	Neodymium 10.22	Tc	Ruthenium 11.3	Rh
W	180.95	74	183.85	75	186.2	190.2
Re	186.2	75	186.2	76	190.2	191.2
Os	190.2	76	190.2	77	191.2	192.2



^{113}In , ^{115}Sn are p-only isotopes?

r-process contribution (*Dillmann et al. 2008, Nemeth et al. 1994*)?

b-process

Claudia Travaglio

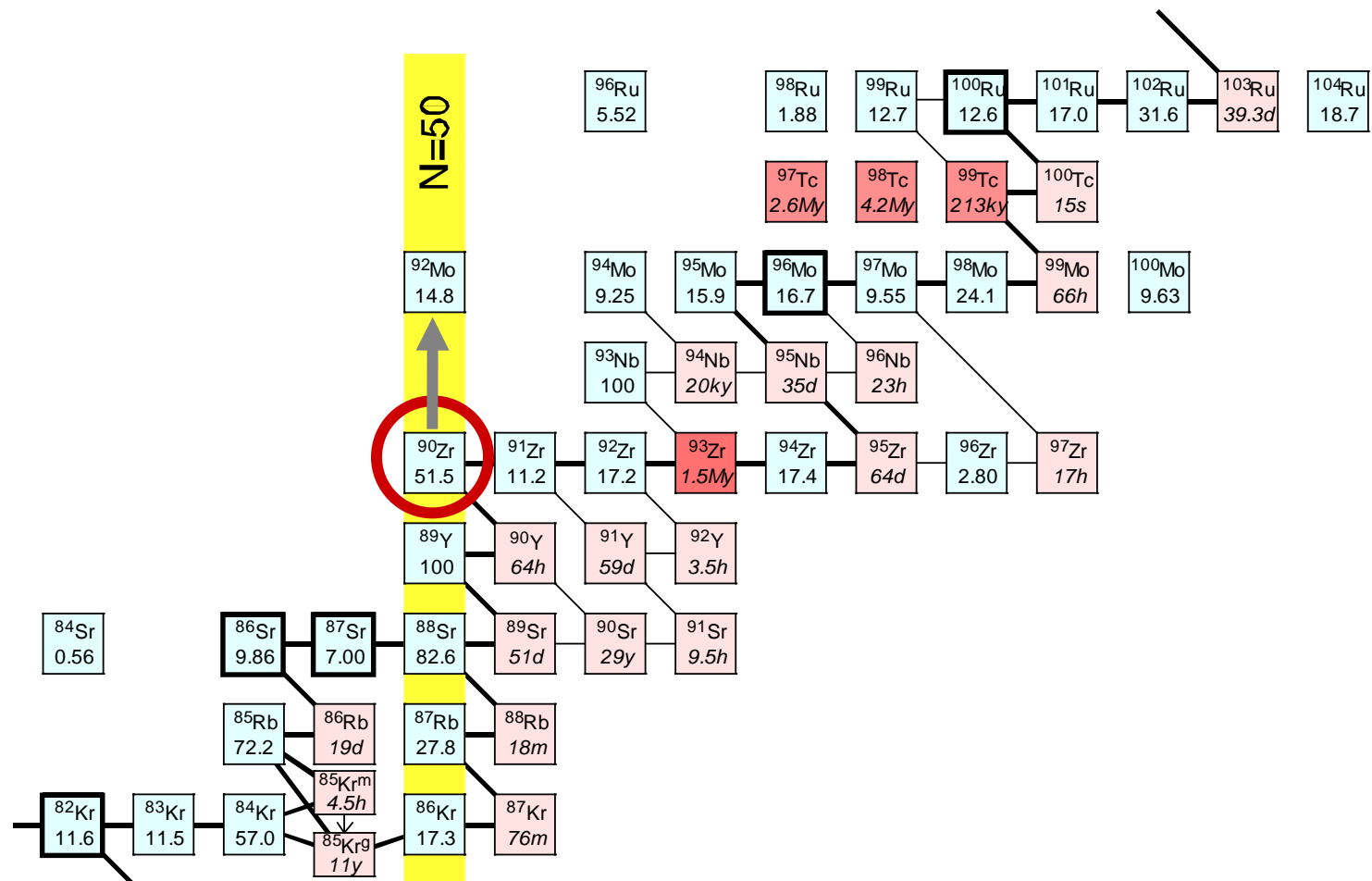
Heidelberg, July 19.-23 2010



90Zr

60% from GCE of s-process

Travaglio et al. 2004; Serminato et al. 2009



+ p-process contribution from SNIa to be taken into account

p-process

Claudia Travaglio

Heidelberg, July 19-23 2010



Future

Nucleosynthesis in accreted mass
(Cristallo, Piersanti et al. in progress)

Sub-Chandrasekhar models
(Roepke et al. at MPA)

Chemical evolution

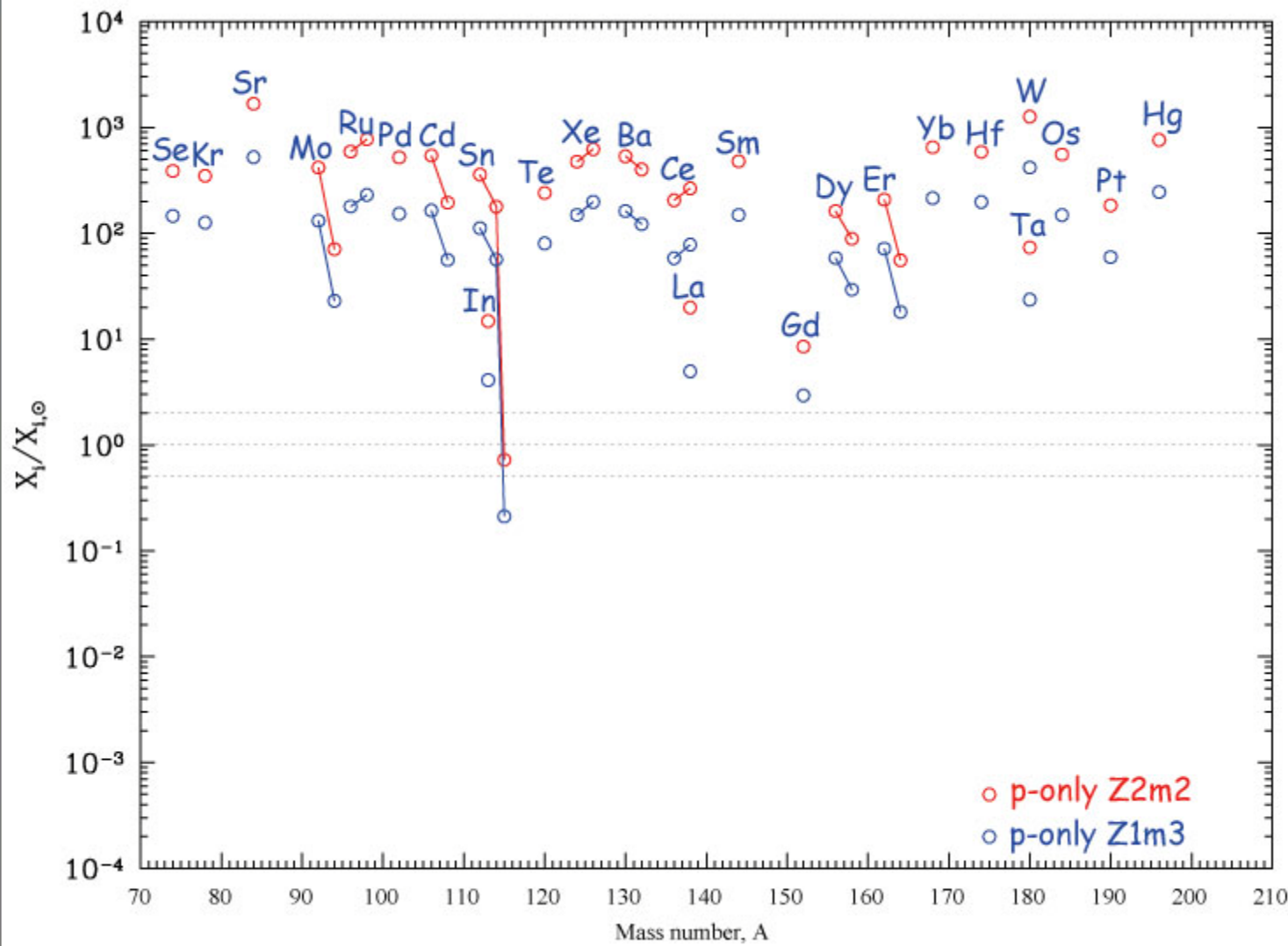
p-process

Claudia Travaglio

Heidelberg, July 19-23 2010



Metallicity study



V	Chromium	Manganese	Iron	Niobium	Molybdenum	Techneium	Ruthenium	Rhenium	Tantalum	Wolfram	Rhenium
Vanadium 6.1	Chromium 7.99	Manganese 7.43	Iron 7.87	Niobium 8.57	Molybdenum 10.22	Techneium (0.48)	Ruthenium 10.3	Rhenium 10.17	Tantalum 180.95	Wolfram 183.85	Rhenium 186.2
92.91	42	95.94	43	(98)	74	75	76	77	74	75	76
4					7						

p-process

Claudia Travaglio

Heidelberg, July 19-23 2010

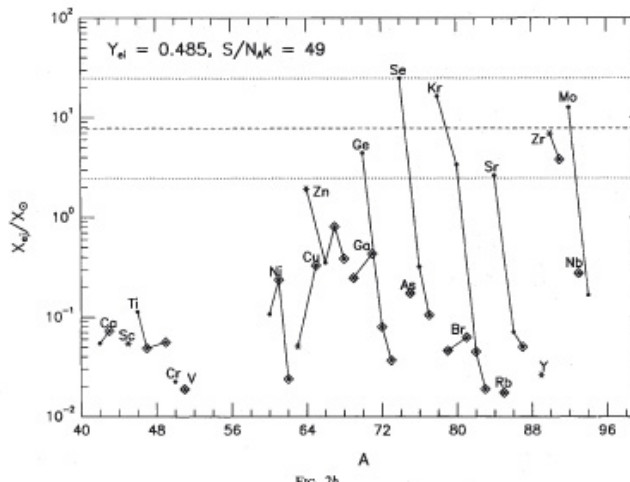
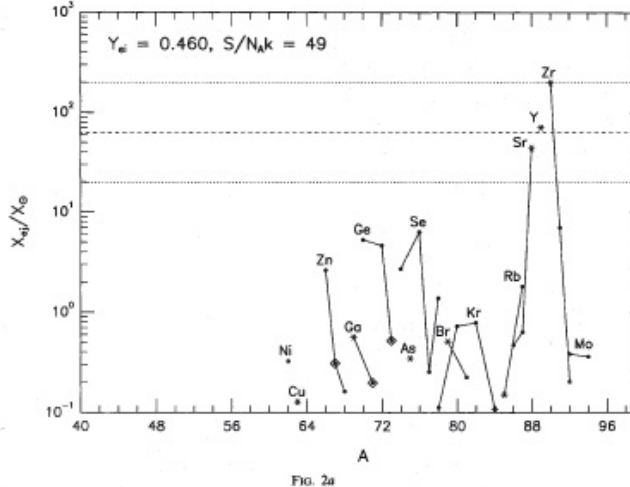
p-process

Claudia Travaglio

Heidelberg, July 19-23 2010



p-process in SNII:



1 the νp -process

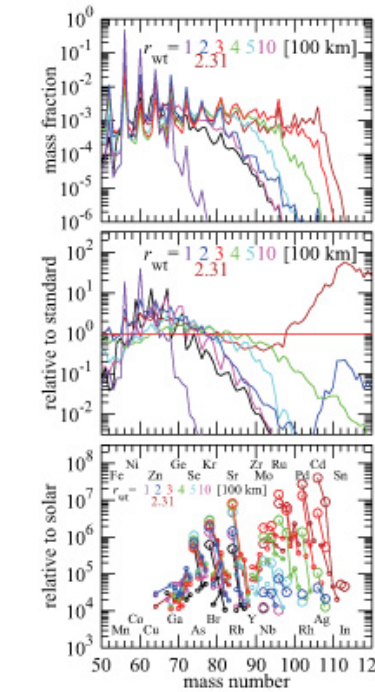


FIG. 2.— Comparison of the nucleosynthetic results for various wind-termination radii r_{wt} . The mass fractions (top) and their ratios (middle) are shown as a function of atomic mass number. The bottom panel shows the abundances of isotopes (connected by a line for a given element) relative to their solar values, where those lower than 10^{-6} are omitted. The color coding corresponds to different values of r_{wt} as indicated in each panel (red is the standard model). The result for the outflow without wind termination is shown in black. In the bottom panel, the names of elements are specified in the upper (even Z) and lower (odd Z) sides at their lightest mass numbers.

This condition continues until the end of their communication.

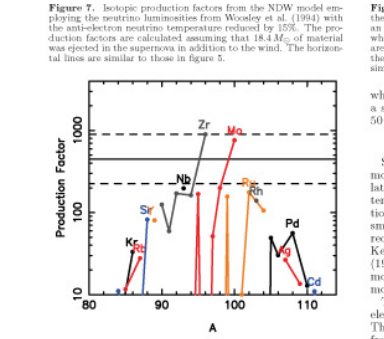


FIGURE 4.— Isotopic production factors from the NDW model employing the neutrino luminosities from Woosley et al. (1994) with an external boundary pressure is specified as described in the text, which results in a wind termination shock. The production factors are calculated assuming that $18.4 M_{\odot}$ of material was ejected in the supernova in addition to the wind. The horizontal lines are similar to those in figure 5.

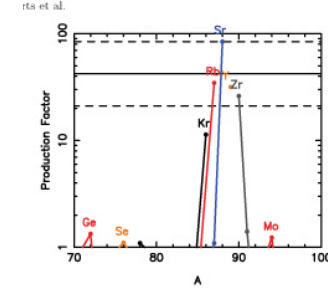


FIGURE 5.— Isotopic production factors from the NDW model employing the neutrino luminosities from Woosley et al. (1994) with an external boundary pressure is specified as described in the text, which results in a wind termination shock. The production factors are calculated assuming that $18.4 M_{\odot}$ of material was ejected in the supernova in addition to the wind. The horizontal lines are similar to those in figure 5.

which r -process nucleosynthesis is expected, but spends a significant amount of time making nuclei in the $N = 50$ closed shell isotones.

4.1.1. Variations in Neutrino Properties

Since the neutrino temperatures from the original model were uncertain, several other models were calculated. One had a reduced (by 15%) electron antineutrino temperature; another had the weak magnetism corrections to the neutrino interaction rates turned off. A smaller antineutrino temperature is more in line with recent calculations of PNS cooling (Pons et al. 1999; Keil et al. 2003). Because the model of Woosley et al. (1994) did not include weak magnetism corrections, our model with weak magnetism corrections turned off is more consistent with the original supernova model.

The production factors for the model with a reduced electron antineutrino temperature are shown in figure 7. The yield of ^{88}Sr is reduced by almost a factor of ten from the base case, while the production factors of ^{85}Y and ^{90}Zr are reduced by a factor of three. In this case, the wind also produces the proton-rich isotopes ^{74}Se , ^{78}Kr , and ^{84}Sr . The coproduction line for lighter elements like oxygen in a $20M_{\odot}$ supernova at solar metallicity around 18, so the wind could contribute to the total nucleosynthesis if the antineutrino temperature was

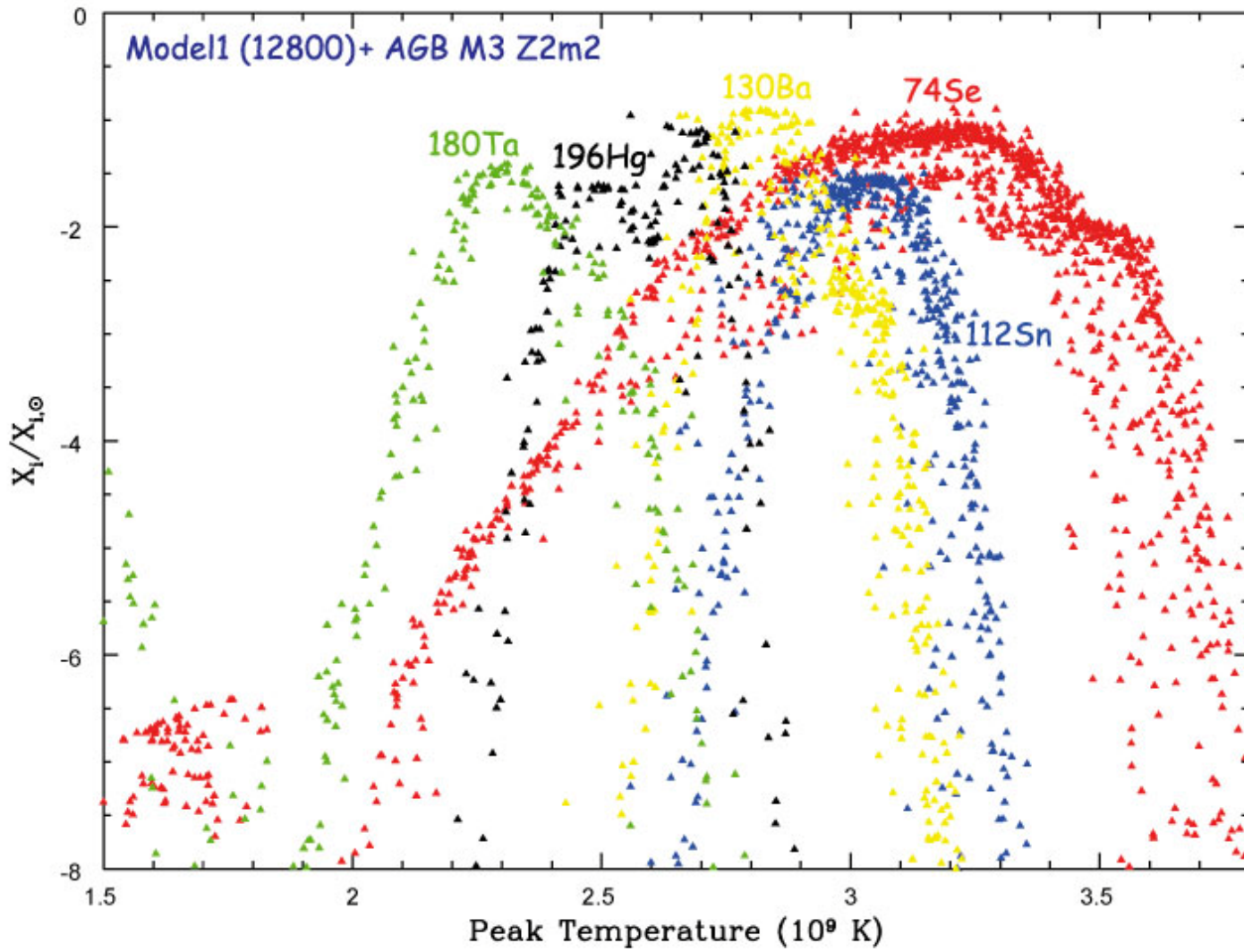
p-process

Claudia Travaglio

Heidelberg, July 19-23 2010



At which T p-process formed?



p-process

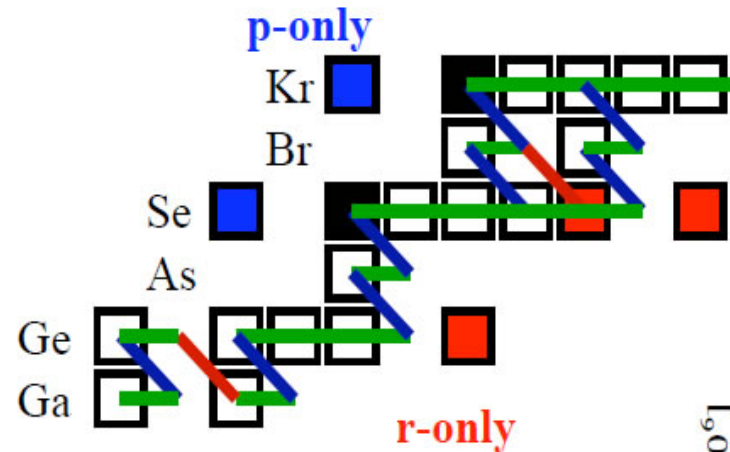
Claudia Travaglio

Heidelberg, July 19-23 2010



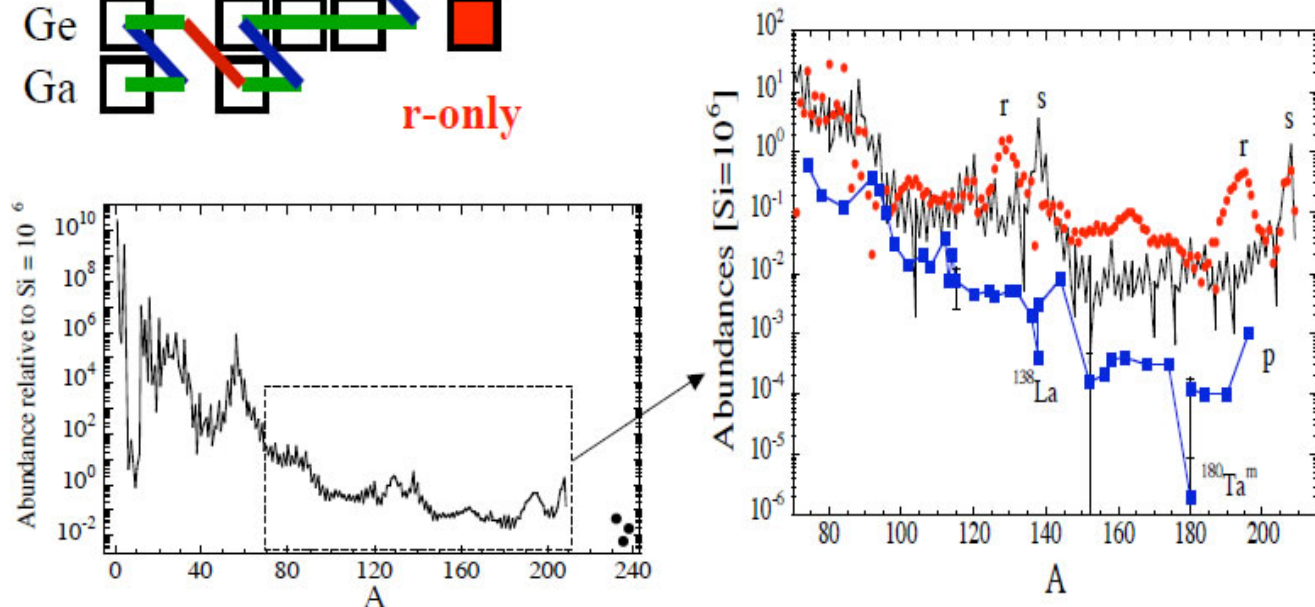
Solar composition

In nature 35 nuclei can be found on the neutron-deficient side of the valley of stability ranging from ^{74}Se and ^{196}Hg , which are shielded against production by n-capture processes.



Separation of the stable nuclei into

- Proton-rich isobar: p-nuclei
- Neutron-rich isobars: r-nuclei
- Isobars at the bottom of the valley of β -stability: s-nuclei



p-process

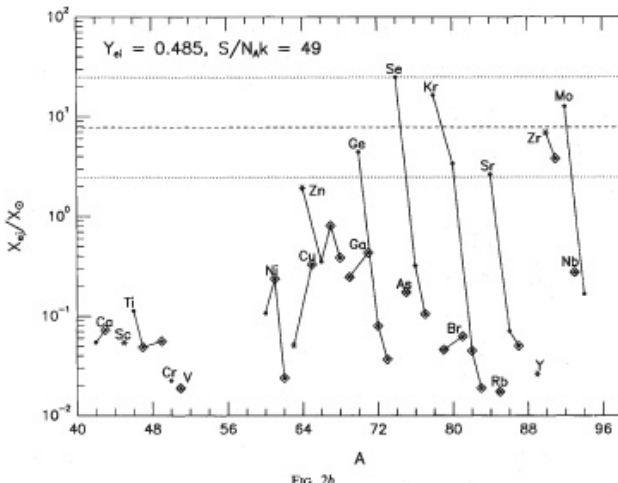
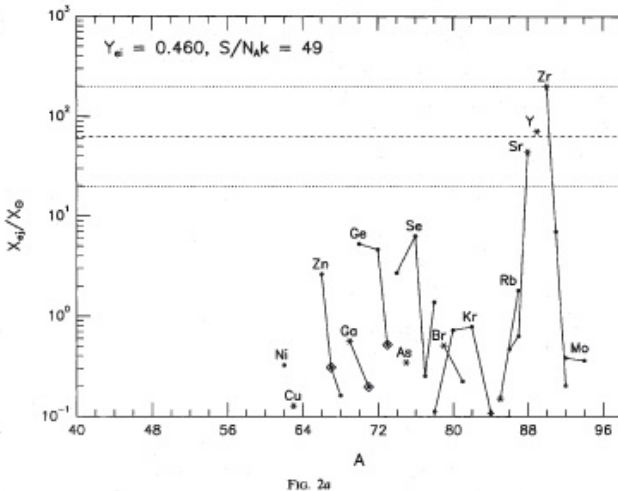
Claudia Travaglio

Heidelberg, July 19-23 2010



p-process

Thielemann et al., 2010



i the ν -process

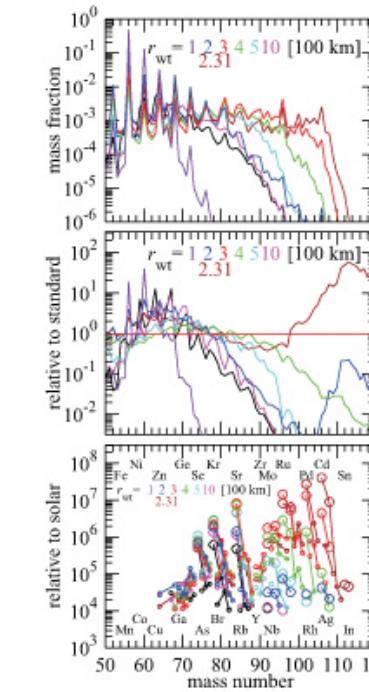


FIG. 2.— Comparison of the nucleosynthetic results for various wind-termination radii r_{wt} . The mass fractions (X_e) and their ratios relative to those for the standard model (middle) are shown as a function of atomic mass number. The bottom panel shows the abundances of isotopes (connected by a line for a given element) relative to their solar values, where those lower than 10^{-6} are omitted. The color coding corresponds to different values of r_{wt} as indicated in each panel (red is the standard model). The result for the outflow without wind termination is shown in black. In the bottom panel, the names of elements are specified in the upper (even Z) and lower (odd A) sides at their lightest mass numbers.

This condition continues until the end of their communication.

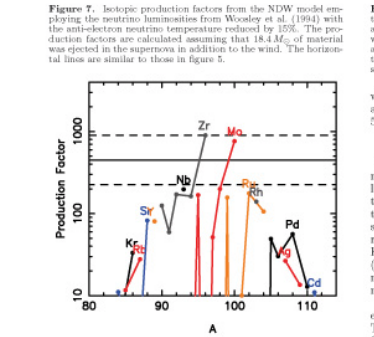


FIGURE 7.— Isotopic production factors from the NDW model employing the neutrino luminosities from Woosley et al. (1994) are used and an external boundary pressure is specified as described in the text, which results in a wind termination radius of 155%. The production factors are calculated assuming that $18.4 M_\odot$ of material was ejected in the supernova in addition to the wind. The horizontal lines are similar to those in figure 5.

3

Wanajo, Janka, Kubono, ApJ submitted

Roberts, Woosley, Hoffman, ApJ Submitted

et al.

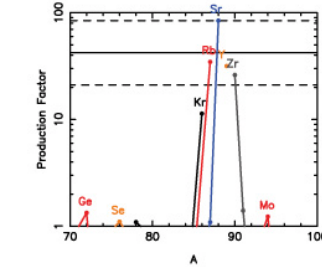


FIGURE 9.— Isotopic production factors from the NDW model employing the neutrino luminosities from Woosley et al. (1994) are used and an external boundary pressure is specified as described in the text, which results in a wind termination radius of 155%. The production factors are calculated assuming that $18.4 M_\odot$ of material was ejected in the supernova in addition to the wind. The horizontal lines are similar to those in figure 5.

which r-process nucleosynthesis is expected, but spends a significant amount of time making nuclei in the N = 50 closed shell isotones.

4.1.1. Variations in Neutrino Properties

Since the neutrino temperatures from the original model were uncertain, several other models were calculated. One had a reduced (by 15%) electron antineutrino temperature; another had the weak magnetism corrections to the neutrino interaction rates turned off. A smaller antineutrino temperature is more in line with recent calculations of PNS cooling (Pons et al. 1999; Keil et al. 2003). Because the model of Woosley et al. (1994) did not include weak magnetism corrections, our model with weak magnetism corrections turned off is more consistent with the original supernova model.

The production factors for the model with a reduced electron antineutrino temperature are shown in figure 7. The yield of ^{88}Sr is reduced by almost a factor of ten from the base case, while the production factors of ^{89}Y and ^{90}Zr are reduced by a factor of three. In this case, the wind also produces the lighter r-process isotopes ^{74}Se , ^{75}Kr , and ^{84}Sr . The coproduction line for lighter elements like oxygen in a $20 M_\odot$ supernova at solar metallicity around 18, so the wind could contribute to the total nucleosynthesis if the antineutrino temperature was